Published in final edited form as:
Stroke. 2014 August ; 45(8): 2335–2341. doi:10.1161/STROKEAHA.114.005975.

Routine clinical evaluation of cerebrovascular reserve capacity using carbogen in patients with intracranial stenosis

Manus J. Donahue, PhD[a,b,c,d,*], **Lindsey Dethrage, BA**[a], **Carlos C. Faraco, PhD**[a], **Lori C. Jordan, MD, PhD**[b], **Paul Clemmons, RN**[e], **Robert Singer, MD**[e], **J Mocco, MD**[f], **Yu Shyr, PhD**[g], **Aditi Desai, MD**[a], **Anne O'Duffy, MD**[b], **Derek Riebau, MD**[b], **Lisa Hermann, MD**[b], **John Connors, MD**[a,f], **Howard Kirshner, MD**[b], and **Megan K. Strother, MD**[a,f]

[a]Radiology, Vanderbilt University, Nashville, TN

[b]Neurology, Vanderbilt University, Nashville, TN

[c]Psychiatry, Vanderbilt University, Nashville, TN

[d]Physics, Vanderbilt University, Nashville, TN

[e]Neurosurgery, Geisel School of Medicine, Dartmouth College, Hanover, NH

[f]Neurosurgery, Vanderbilt University, Nashville, TN

[g]Center for Quantitative Sciences, Vanderbilt University, Nashville, TN

Abstract

Background and Purpose—A promising method for identifying hemodynamic impairment that may serve as a biomarker for stroke risk in patients with intracranial (IC) stenosis is cerebrovascular reactivity (CVR) mapping using non-invasive MRI. Here, abilities to measure CVR safely in the clinic using hypercarbic hyperoxic (carbogen) gas challenges, which increase oxygen delivery to tissue, are investigated.

Methods—In sequence with structural and angiographic imaging, blood-oxygenation-level-dependent (BOLD) carbogen-induced CVR scans were performed in patients with symptomatic IC stenosis (n=92) and control (n=10) volunteers, with a subgroup of patients (n=57) undergoing cerebral blood flow-weighted (CBFw) pseudo-continuous arterial spin labeling (pCASL) CVR. Subjects were stratified for four sub-studies: to evaluate relationships between (i) carbogen and hyercarbic normoxic (HN) CVR in healthy tissue (n=10), (ii) carbogen CBF CVR and BOLD CVR in IC stenosis patients (n=57), (iii) carbogen CVR and clinical measures of disease in patients with asymmetric IC atherosclerotic (n=31) and moyamoya (n=29) disease, and (iv) the CVR scan and immediate and longer-term complications (n=92).

Results—Non-invasive BOLD carbogen-induced CVR values correlate with (i) lobar HN gas stimuli in healthy tissue (R=0.92; P<0.001), (ii) carbogen-induced CBF CVR in IC stenosis patients (R=0.30–0.33; P<0.012), and (iii) angiographic measures of disease severity both in

[*]Corresponding Author/Permanent Address: Manus Donahue, VUIIS,1161 21st Avenue South, Nashville, TN, 37232, Tel: 615.322.8350, Fax:615.322.0734, mj.donahue@vanderbilt.edu.

Conflict of Interest/Disclosure
Yu Shyr is a consultant for GlaxoSmithKline, AduroBiotech Inc., and Janssen.

atherosclerotic and moyamoya patients after appropriate processing. No immediate stroke-related complications were reported in response to carbogen administration; longer-term neurological events fell within the range for expected events in this patient population.

Conclusions—Carbogen-induced CVR elicited no added adverse events and provided a surrogate marker of cerebrovascular reserve consistent with IC vasculopathy.

Keywords

cerebrovascular reserve; BOLD; stenosis; stroke

Introduction

Recent studies have shown high two-year ischemic stroke rates of approximately 20% in symptomatic intracranial (IC) stenosis patients[1]. Despite this high stroke rate, risks related to endovascular revascularization, particularly in light of recent improvements in medical management, have led to recent halting of two major IC stent trials for symptomatic IC stenosis[2, 3]. Waning interest in IC stenting may ignore a subset of high-risk patients who have true hemodynamic instability, a finding associated with a 60.7% three-year recurrent stroke rate in one prospective study[4]. The critical barrier to better informing treatment decisions rests with a relative lack of abilities to measure the wide range of cerebral hemodynamic compromise possible, and furthermore to use this information to evaluate how evolution of hemodynamic changes portend personalized stroke risk.

Reductions in cerebral perfusion pressure can be compensated for by increases in parenchymal cerebral blood volume (CBV) and cerebral blood flow (CBF)[5, 6]. Cerebrovascular reactivity (CVR), or the ability of vessels to regulate CBF and CBV, provides an indicator of the cerebrovascular reserve and potentially how near tissue is to failing to meet hemodynamic demand. The magnitude and response time of CVR, assessed using exogenous vasodilator agents, has been demonstrated to correlate variably with stroke risk and symptomatology[7].

CVR measurements induced by changes in blood oxygenation secondary to hypercarbic gas administration are increasingly utilized, primarily in research settings[8, 9] whereby elevated CO_2 levels (4–6%) are administered, most commonly with a balance of medical-grade atmospheric air ($21\%O_2/74\%N_2$). This leads to increases in the arterial partial pressure of CO_2 ($PaCO_2$), CBF, and CBV, and in turn an increase in blood oxygenation in capillaries and veins (Figure 1A). This small increase in oxy-hemoglobin (HbO_2), relative to deoxy-hemoglobin (dHb), manifests as an increase in T_2*-weighted MRI signal (i.e., the blood-oxygenation-level-dependent, BOLD, effect). Two factors have slowed BOLD CVR mapping in clinical stroke imaging. First, the safety of such hypercarbic gas mixtures is unclear in patients with ischemia, as challenging vasculature operating near reserve capacity may exacerbate symptoms or elicit new neurological events. Second, hypercarbic gas administration frequently involves unique setups that utilize mechanisms of end-tidal forcing or similar procedures[8, 10]. While well-controlled, these systems may be impractical for routine clinical utilization.

Alternatively, carbogen, consisting of hypercarbia with a balance of oxygen (i.e., 5%CO_2/95%O_2: hypercarbic hyperoxia) can also induce changes in CVR, while also increasing oxygen transport to tissue[11]. However, transient hyperoxia may influence metabolism and will increase in partial pressure of arterial oxygen (PaO_2), and arterial (Y_a) and venous (Y_v) oxygen saturation, increasing blood oxygenation unrelated to CVR. It remains unclear how carbogen-induced CVR measurements correlate with angiographic and clinical impairment in patients with IC stenosis. This issue is fundamental, as carbogen administration is in principle a more clinically feasible and safer challenge than hypoxia or hypercarbic normoxia.

We enrolled patients with IC stenosis over a three-year window and recorded carbogen CVR measurements obtained in a clinical radiological unit using standard gas delivery equipment available at most hospitals with four main aims: to (i) characterize differences in hypercarbic normoxic and carbogen CVR in healthy parenchyma, (ii) assess the relationship between carbogen-induced CBF CVR and BOLD CVR in ischemic and healthy tissue, (iii) correlate carbogen CVR with standard clinical measures of disease, and (iv) provide preliminary data on intrascan and longer-term (6–12 month) complications resulting from carbogen CVR imaging.

Methods

Ethical considerations

All study components were compliant with HIPAA and the Helsinki Declaration and approved by the local Institutional Review Board. Subjects were enrolled between December 2011 and March 2014 and included healthy volunteers (n=10), patients with confirmed-or-suspected IC stenosis (n=92), and follow-up scans in a subgroup of patients (n=33). Patients were enrolled as part of the Vanderbilt Assessment of Multimodal Mri in Patients at-Risk for stroke with Intracranial Stenosis (VAMMPRIS) trial and provided informed, written consent for this prospective study. This study included four components with differing inclusion/exclusion criteria (additional details provided as Supplemental Material):

(i) Hypercarbic gas comparison—The purpose of this study was to contrast hypercarbic normoxic and carbogen-induced BOLD CVR in healthy volunteers (Table 1; n=10). *Experiment.* All MRI measurements were performed at 3.0T (Philips). CVR was assessed in response to delivery (12 L/min) of carbogen gas (5%CO_2/95%O_2) administered through a non-rebreathing oxygen facemask (Salter Labs, Ref:8130). Physiological monitoring was achieved using an In Vivo Research Inc. (3150 MRI) device and Millenia Vital Systems Monitoring System (3155MVS). Monitored parameters included heart rate, blood pressure, Y_a, and $EtCO_2$ response ($\Delta EtCO_2$) (Salter Labs; Ref:400F). The stimulus paradigm consisted of two blocks of 3 min carbogen administration and hypercarbic normoxia (5%CO_2/21%O_2/74%N_2) interleaved with 3 min of medical grade air (~21%O_2/ ~79%N_2: normocarbic normoxia). Stimulus order was randomized between subjects. Whole-brain BOLD images (TE=35 ms) were acquired with spatial resolution=3.5 mm isotropic. *Analysis.* All data were corrected for motion and baseline drift using standard

affine-correction algorithms and spatially smoothed (full-width-half-maximum=3mm)[12]. CVR was calculated according to relative signal changes ($\Delta S/S_0$), defined as the mean difference in the signal during the final 90s of each stimulus block and baseline block, divided by the mean signal during the final 90s of the baseline block. To allow for comparison between subjects, all data were co-registered to a standard T_1-weighted atlas and lobar CVR was recorded (Supplementary Figure I). Pearson correlation and linear regression were performed for CVR measures derived from the two stimuli.

(ii) CBF vs. BOLD CVR—The purpose of this study was to assess the extent to which carbogen-induced BOLD CVR measures correlated with carbogen-induced CBF CVR derived from independent CBF measures obtained from arterial spin labeling (ASL). *Experiment.* A subgroup (Table 1; n=57) of patients scans had BOLD and ASL CVR measurements recorded in the same scan session. The BOLD protocol was as outlined above except without the hypercarbic normoxia challenge. For ASL, a pseudo-continuous (pCASL) sequence was employed with 1.6s labeling pulse train, followed by post-labeling delay of 1.525s. The gas paradigm consisted of approximately 5 min room air breathing and 5 min carbogen. *Analysis.* BOLD data were post-processed as described above. pCASL data were surround-subtracted and normalized by M_0 to generate CBF-weighted maps, spatially smoothed to match the BOLD post-processing, and CBF was quantified upon application of the solution of the flow-modified Bloch equation assuming a blood water T_1 reduction from 1.6s to 1.4s and bolus arrival time (BAT) reduction of 5% for the transition from room air to carbogen. CBF reactivity was defined as CBF change normalized by baseline CBF ($\Delta CBF/CBF_0$).

(iii) BOLD CVR and lateralizing disease—The purpose of this study was to contrast carbogen-induced BOLD CVR with angiographic and clinical measures of disease severity in patients with atherosclerotic and moyamoya IC stenosis. *Experiment.* We focused on lateralizing IC stenotic disease. Inclusion criterion for atherosclerotic patients was ipsilateral IC stenosis≥50%. Exclusion criterion was cervical stenosis>70%. In moyamoya subjects, inclusion criterion was at least one hemisphere with modified Suzuki Score (mSS)>0. These criteria led to 29 moyamoya and 31 atherosclerotic patients meeting inclusion criteria. Stenosis degree of major IC and cervical vessels was classified by a board-certified neuroradiologist (MKS; experience=13 years). In patients with clinically-confirmed idiopathic moyamoya disease, mSS was calculated separately in right and left hemispheres[13]. Additional stroke risk factors including smoking status, diabetes, prior infarct, body-mass-index (BMI), cardiovascular events, and age were recorded, along with anti-platelet and anti-coagulant medications. The BOLD imaging protocol was identical as outlined in *ii. Analysis*. CVR was calculated in two different ways. First, relative signal changes, as outlined in the *hypercarbic gas comparison* were calculated. Second, z-statistics were calculated. Here, the carbogen waveform was used in the FMRIB Software Library (FSL)[12] design matrix and a corresponding parameter estimate image was calculated, which corresponded to how strongly that stimulus fits the data. The parameter estimate map was converted to a t-statistic image by normalizing by the standard error. The t-image was then transformed into a z-statistic. Signal change and z-statistic maps were co-registered to a standard T_1-weighted brain atlas. For IC atherosclerotic patients, “affected” hemispheres

were defined as hemispheres with IC stenosis≥50%, and "contralateral" hemispheres were defined as hemispheres with no IC stenosis ≥50%. In moyamoya patients, hemispheres were oriented by higher mSS ("affected" hemispheres) vs. lower mSS ("contralateral" hemispheres). The co-registered CVR maps were oriented: radiological right=affected and radiological left=contralateral. CVR was calculated in 11 brain regions. A Student's t-test assessed significance between affected and contralateral hemispheres. A general linear model, including major stroke risk factors as defined by the Framingham study[14], was also applied to understand the extent to which different risk factors contributed to lateralizing CVR.

(iv) Safety—The purpose of this study was to record any immediate (during the scan) and longer-term (approximately one-year follow-up) complications that arose in patients participating in this study. *Experiment.* All patient scans were analyzed, which included 92 separate patient scans plus 33 follow-up scans. Of these 125 total scans, immediate follow-up was provided from all patients scans and additional longer-term follow-up was performed after approximately one year. For short and long-term follow-up, a stroke research nurse contacted the patient by phone and conducted a questionnaire. Findings were interpreted by a board-certified stroke neurologist (LCJ). Complications were classified as either (i) new stroke-like symptoms, (ii) stroke-like symptoms that began before the CVR scan, or (iii) symptoms of non-stroke origin. *Analysis.* Results of the safety questionnaire were recorded and long-term complication rates were contrasted with expected neurovascular event rates in this patient population[1].

Results

(i) Hypercarbic gas comparison

Figure 1A shows representations of fractional changes in HbO_2 relative to dHb at baseline and for different stimuli. Figure 1B shows that BOLD $\Delta S/S_0$, normalized by $\Delta EtCO_2$, provides similar contrast for the two gas stimuli, albeit with different intensity. Figure 1C demonstrates that the two measures correlate tightly ($P<0.05$) across all brain lobes. Figure 1D demonstrates that CVR trends between brain regions are similar for the two gas stimuli. These data are consistent with carbogen BOLD CVR providing similar information to hypercarbic normoxic BOLD CVR, however with an additional contribution from increased oxygen saturation secondary to hyperoxia. The best fit line to these data was found to provide a slope of 2.53 (intercept=0.00).

(ii) CBF vs. BOLD CVR

Figure 2A shows baseline and CBF reactivity (upper) and BOLD reactivity (Z-stat/$\Delta EtCO_2$ and $\Delta S/S_0/\Delta EtCO_2$) for the same patients (Table 1; Supplementary Table I; n=57). In Figure 2B, the relationships between BOLD and CBF CVR for all gray matter in affected and contralateral brain hemispheres are shown. Correlations are found between both measures of CVR for all scenarios except BOLD Z-stat vs. CBF CVR in the contralateral hemisphere.

(iii) BOLD CVR and lateralizing disease

CVR maps calculated according to signal changes ($\Delta S/S_0$), T-stat, and Z-stat are shown in Figure 3. Figure 3A,B shows data for atherosclerotic (Table 1; Supplementary Table II; n=31) patients and Figure 3C,D shows data for moyamoya (Table 1; Supplementary Table III; n=29) patients. These data demonstrate that in atherosclerotic patients, CVR is consistently reduced, with the exception of the occipital lobes and cerebellum, in the hemisphere of the stenotic vessel when BOLD Z-statistics are used for CVR determination. Sparing of occipital lobes and cerebellum is consistent with the predominantly anterior circulation stenosis in our IC atherosclerosis patients (19% had posterior circulation stenosis and 13% had only posterior circulation involvement). Lateralizing CVR is less apparent when $\Delta S/S_0$ is considered, or when moyamoya patients are considered, consistent with the bilateral nature of moyamoya disease. A multivariate analysis was performed to understand the extent that additional stroke-risk factors contributed to lateralizing CVR (Table 2). It was found that age, but not smoking or diabetes, contributed significantly to lateralizing disease in atherosclerotic patients. In moyamoya patients, it was found that mSS, but not age, smoking, or diabetes were significant additional predictors of lateralizing CVR. Figure 4 shows multi-modal data from an (A) atherosclerotic and (B) moyamoya patient, demonstrating how CVR maps can complement standard clinical imaging.

Safety

Table 1 (lower) shows safety results. No patients reported stroke-like symptoms in the immediate follow up; 2/125 (1.6%) experienced claustrophobia during the scan. For the longer-term follow-up (median=372 days), 5.0% of patients had stroke-like symptoms as determined by a neurologist (LCJ), which is within the range of expected neurovascular events for this population[1]. All symptoms are documented in Supplementary Table IV.

Discussion

The major findings from this study are that non-invasive CVR values derived from carbogen stimuli correlate (i) with hypercarbic normoxic gas stimuli in healthy tissue, (ii) with CBF CVR to carbogen in affected and contralateral brain hemispheres of IC stenosis patients, and (iii) with angiographic measures of disease severity both in atherosclerotic and moyamoya patients after appropriate processing (Z-statistic). Finally, (iv) we provide preliminary information showing no immediate or short-term stroke-related complications from this protocol, and longer-term complications that fall within the expected range of neurovascular events for this patient population.

These findings provide the foundation for non-invasively measuring cerebral hemodynamic compromise in IC stenosis patients, which may provide a marker for stroke risk. Following the SAMMPRIS trial[1], management for patients with IC stenosis remains unclear. Although the risks of endovascular stenting exceeded the risks for aggressive medical management in this trial, other trials suggest a subset of subjects with true hemodynamic instability have much high rates of stroke[4]. MRI measurements of CVR represent a promising class of screening procedures to identify hemodynamic instability. Traditional vasodilatory agents, including acetazolamide and remifentanil, have been used to elicit changes in CVR, and

monitored using BOLD and CBF-weighted techniques, however these agents are not universally safe. By contrast, the carbogen stimulation increases oxygen delivery to tissue, and can be applied without the same concerns related to dose-restrictions. Additionally, unlike PET and SPECT, MRI has no ionizing radiation exposure.

The confound of using carbogen in conjunction with non-invasive MRI measures is that carbogen increases blood oxygenation level in a manner that is non-specific to CVR, and also hyperoxia reduces blood water T_1. A recent study found no correlation between BOLD and CBF CVR in response to carbogen in a smaller (n=16) population of healthy adults[15]. Several differences between this study and ours should be noted. First, we used an ASL post-labeling delay (PLD) of 1.525s, approximately consistent with recent recommendations from the International-Society-For-Magnetic-Resonance-In-Medicine ASL study section[16]. In the above study[15], a much shorter PLD=800 ms was used, which drastically increases sensitivity to intravascular blood water relative to CBF. Second, the small sample size and focus on healthy tissue only in the above study[15] limits the range of flow-volume coupling scenarios, thereby limiting the power available to find significant correlations. This is consistent with our Figure 2, whereby stronger relationships between BOLD and CBF CVR are observed in affected regions, where a broader range of flow-volume coupling is present. We do agree that hypercarbic normoxia is a simpler challenge that is more straightforward to interpret, yet this method has met resistance for clinical use owing to concerns related to hypercarbic administration in patients with cerebrovascular impairment.

There are several limitations. First, it is unclear whether hyperoxia from carbogen influences metabolism and perfusion. Small vasoconstrictive effects are likely present in hyperoxia, however these effects have been measured to be small relative to the vasodilatory effect from hypercarbia[11]. Additionally, while carbogen is believed to be primarily isometabolic in healthy adults, it is unclear whether ischemic tissue may upregulate $CMRO_2$ during periods of increased oxygen delivery. Second, multiple factors contribute to stroke risk, and given the sample size of the clinical components of this study, n=57 (study ii), n=60 (study iii) and n=125 (study iv), not all could be controlled for. We chose to restrict inclusion criteria to a relatively homogeneous population of asymmetric IC stenosis patients with no cervical stenosis >70%, and we perform multivariate analysis of the major stroke risk factors only (Supplementary Material). We did not control for dolichoectasia, although patients with dolichoectasia and related cerebrovascular morphological abnormalities of cervical vessels may have increased stroke risk[17, 18]. Unfortunately, our patients do not routinely undergo carotid echo-color Doppler and only a subset of our patients had cerebral angiography; larger studies that assess the relationship of CVR with other stroke risk factors may benefit by incorporating separate measurements of dolichoectasia. Finally, the purpose of this study was to outline relationships between carbogen-induced BOLD CVR and more standard imaging measures including CBF, vascular stenosis, and hypercarbic normoxic CVR in a relatively controlled cohort (asymmetric IC stenosis) of patients, as well as to provide preliminary safety information on this protocol. Ongoing work in which more patients are enrolled and monitored longitudinally should provide information as to whether characteristics of such contrast has prognostic utility.

Conclusions

Results provide an exemplar for how CVR changes in response to carbogen stimulation in patients with cerebrovascular disease, and could provide an avenue for using this stimulus in clinical scenarios.

Supplementary Material

Refer to Web version on PubMed Central for supplementary material.

Acknowledgments

Sources of funding

NIH/NINDS:5R01NS078828

References

1. Holmstedt CA, Turan TN, Chimowitz MI. Atherosclerotic intracranial arterial stenosis: risk factors, diagnosis, and treatment. Lancet Neurol. 2013; 12:1106–1114. [PubMed: 24135208]
2. Derdeyn CP, Chimowitz MI, Lynn MJ, Fiorella D, Turan TN, Janis LS, et al. Aggressive medical treatment with or without stenting in high-risk patients with intracranial artery stenosis (SAMMPRIS): the final results of a randomised trial. Lancet. 2014; 383:333–341. [PubMed: 24168957]
3. Zaidat OO, Castonguay AC, Fitzsimmons BF, Woodward BK, Wang Z, Killer-Oberpfalzer M, et al. Design of the Vitesse Intracranial Stent Study for Ischemic Therapy (VISSIT) trial in symptomatic intracranial stenosis. J Stroke Cerebrovasc Dis. 2013; 22:1131–1139. [PubMed: 23261207]
4. Mazighi M, Tanasescu R, Ducrocq X, Vicaut E, Bracard S, Houdart E, et al. Prospective study of symptomatic atherothrombotic intracranial stenoses: the GESICA study. Neurology. 2006; 66:1187–1191. [PubMed: 16636236]
5. Liebeskind DS, Cotsonis GA, Saver JL, Lynn MJ, Turan TN, Cloft HJ, et al. Collaterals dramatically alter stroke risk in intracranial atherosclerosis. Ann Neurol. 2010; 69:963–974. [PubMed: 21437932]
6. Derdeyn CP, Videen TO, Yundt KD, Fritsch SM, Carpenter DA, Grubb RL, et al. Variability of cerebral blood volume and oxygen extraction: stages of cerebral haemodynamic impairment revisited. Brain. 2002; 125:595–607. [PubMed: 11872616]
7. Donahue MJ, Strother MK, Hendrikse J. Novel MRI approaches for assessing cerebral hemodynamics in ischemic cerebrovascular disease. Stroke. 2012; 43:903–915. [PubMed: 22343644]
8. Wise RG, Pattinson KT, Bulte DP, Chiarelli PA, Mayhew SD, Balanos GM, et al. Dynamic forcing of end-tidal carbon dioxide and oxygen applied to functional magnetic resonance imaging. J Cereb Blood Flow Metab. 2007; 27:1521–1532. [PubMed: 17406659]
9. Yezhuvath US, Lewis-Amezcua K, Varghese R, Xiao G, Lu H. On the assessment of cerebrovascular reactivity using hypercapnia BOLD MRI. NMR Biomed. 2009; 22:779–786. [PubMed: 19388006]
10. Mandell DM, Han JS, Poublanc J, Crawley AP, Stainsby JA, Fisher JA, et al. Mapping cerebrovascular reactivity using blood oxygen level-dependent MRI in Patients with arterial steno-occlusive disease: comparison with arterial spin labeling MRI. Stroke. 2008; 39:2021–2028. [PubMed: 18451352]
11. Ashkanian M, Gjedde A, Mouridsen K, Vafaee M, Hansen KV, Ostergaard L, et al. Carbogen inhalation increases oxygen transport to hypoperfused brain tissue in patients with occlusive carotid artery disease: increased oxygen transport to hypoperfused brain. Brain Res. 2009; 1304:90–95. [PubMed: 19782665]

12. Jenkinson M, Beckmann CF, Behrens TE, Woolrich MW, Smith SM. Fsl. Neuroimage. 2012; 62:782–790. [PubMed: 21979382]

13. Donahue MJ, Ayad M, Moore R, van Osch M, Singer R, Clemmons P, et al. Relationships between hypercarbic reactivity, cerebral blood flow, and arterial circulation times in patients with moyamoya disease. J Magn Reson Imaging. 2013; 38:1129–1139. [PubMed: 23440909]

14. D'Agostino RB, Wolf PA, Belanger AJ, Kannel WB. Stroke risk profile: adjustment for antihypertensive medication. The Framingham Study. Stroke. 1994; 25:40–43. [PubMed: 8266381]

15. Hare HV, Germuska M, Kelly ME, Bulte DP. Comparison of CO2 in air versus carbogen for the measurement of cerebrovascular reactivity with magnetic resonance imaging. J Cereb Blood Flow Metab. 2013; 33:1799–1805. [PubMed: 23921896]

16. Alsop, DC.; Detre, JA.; Golay, X.; Gunther, M.; Hendrikse, J.; Hernandez-Garcia, L., et al. Recommended implementation of arterial spin-labeled perfusion MRI for clinical applications: A consensus of the ISMRM perfusion study group and the European consortium for ASL in dementia. [published online ahead of print date]. Magn Reson Med. 2014 Apr 8. http://onlinelibrary.wiley.com/doi/10.1002/mrm.25197/pdf

17. Matteo Ciccone M, RKS, Scicchitano P, Cortese F, Salerno C, Berchialla P, et al. Dolichocarotids: echo-color Doppler evaluation and clinical role. J Atheroscler Thromb. 2014; 21:56–63. [PubMed: 24025702]

18. Ciccone MM, Scicchitano P, Palumbo V, Cortese F, Valecce R, Dentamaro I, et al. Dolichocarotids and dilated cardiomyopathy: is there a relationship? Int J Cardiol. 2012; 158:123–125. [PubMed: 22560943]

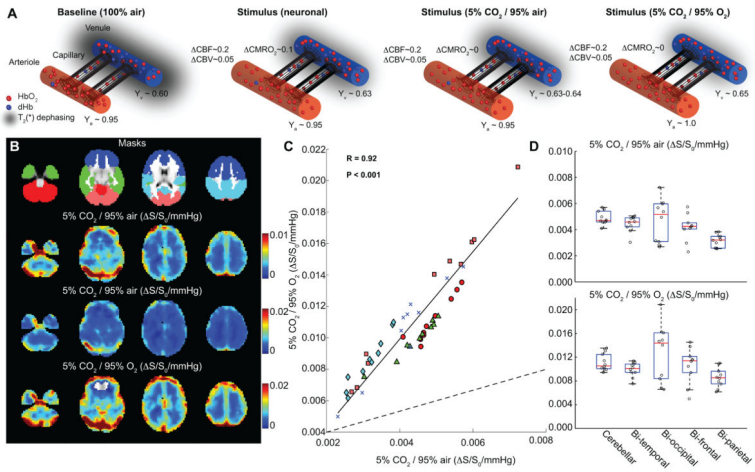

Figure 1. Hypercarbic gas comparison

(A) Graphical representations of fractional changes in oxy-hemoglobin (HbO_2) relative to deoxy-hemoglobin (dHb) at baseline and for different stimuli. For neuronal stimuli, cerebral blood flow (CBF), cerebral blood volume (CBV) and the cerebral metabolic rate of oxygen consumption ($CMRO_2$) all increase, causing a small increase in venous oxygenation (Y_v) in veins. For 5%CO_2/95%air, CBF and CBV increase only. For hypercarbic hyperoxia (i.e., carbogen; 5%CO_2/95%O_2), CBF and CBV increase, however increases in the partial pressure of arterial oxygen will lead to elevation of arterial (Y_a) and Y_v, increasing the BOLD effect in a manner non-specific to cerebrovascular reactivity (CVR). (B) Signal changes ($\Delta S/S_0$) normalized by change in end-tidal CO_2 for the different gas stimuli for healthy volunteers; the hypercarbic normoxic maps have been scaled for maximal contrast and identically to carbogen stimuli maps (Table 1; n=10). (C) The hypercarbic normoxic $\Delta S/S_0$/mmHg is smaller than the carbogen $\Delta S/S_0$/mmHg as expected, however the two measures correlate tightly ($P<0.05$) across all brain lobes; colors denote different lobes shown in (B; Masks). Dashed line=line of unity; solid line=best fit line to data. The boxplot in (D) also demonstrate that relative $\Delta S/S_0$ between brain regions vary similarly for the two gas stimuli. These data are consistent with carbogen BOLD CVR providing similar information to hypercarbic normoxic BOLD CVR, however with an additional contribution from increased oxygen saturation secondary to hyperoxia.

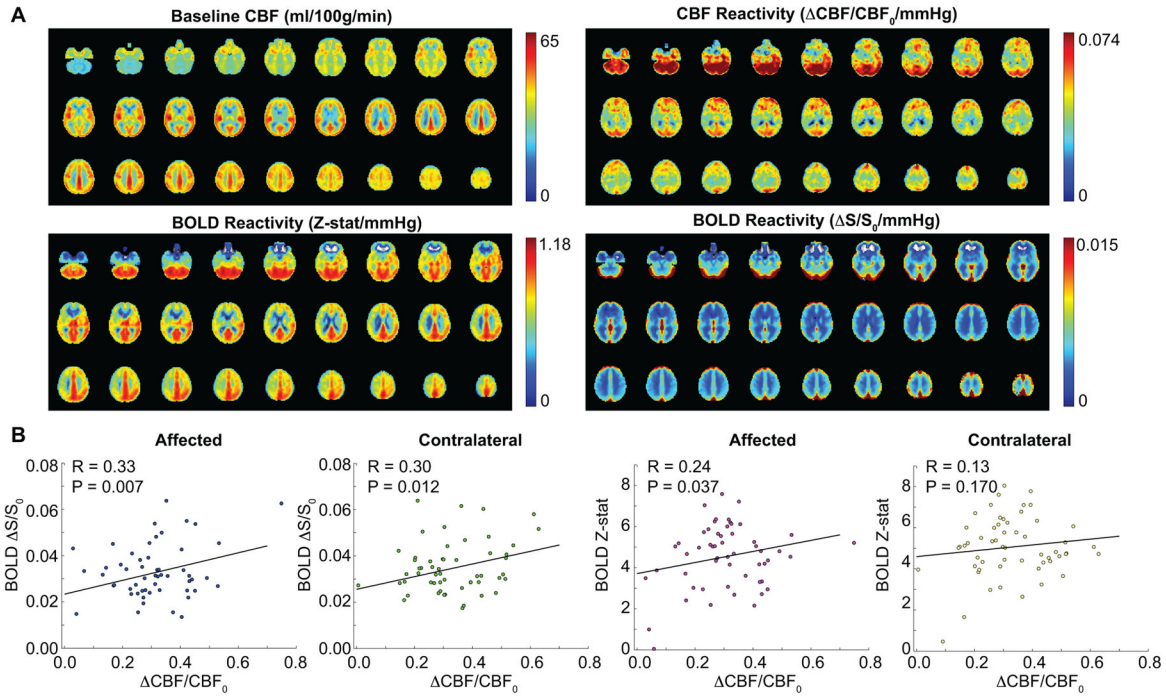

Figure 2. (ii) Cerebral blood flow (CBF) vs. blood oxygenation level-dependent (BOLD) cerebrovascular reactivity (CVR)

(A) Baseline and CBF CVR (upper) and BOLD CVR (Z-stat/mmHg and $\Delta S/S_0$/mmHg) for the same patients (Table 1; n=57). (B) The relationship between BOLD and CBF CVR for all gray matter in affected and contralateral hemispheres. Correlations are found between both measures of CVR for all scenarios except for BOLD Z-stat vs. CBF CVR in contralateral hemisphere.

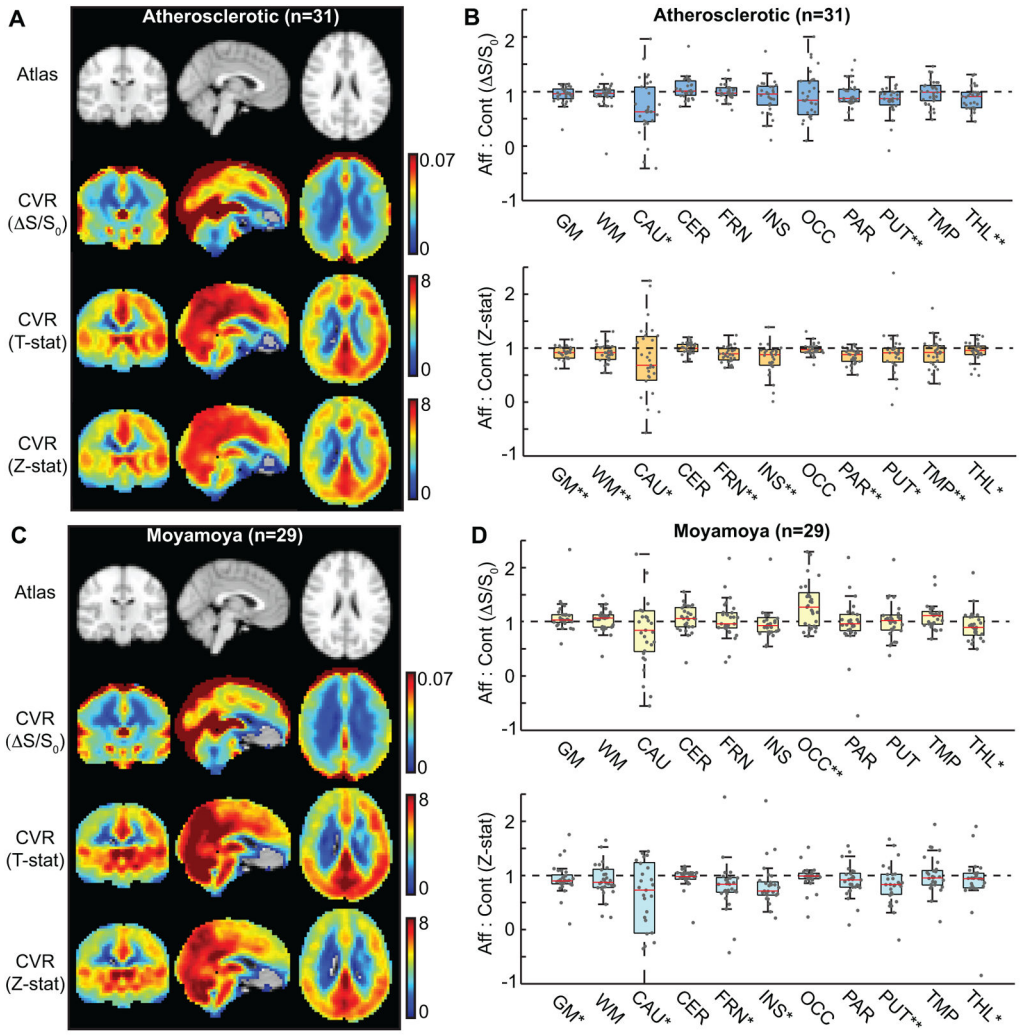

Figure 3. Blood oxygenation level-dependent (BOLD) cerebrovascular reactivity (CVR) and lateralizing disease

CVR maps calculated according to signal changes ($\Delta S/S_0$), T-statistic (T-stat), and Z-statistic (Z-stat). Maps for affected:contralateral ratios for (A,B) atherosclerotic (n=31) and (C,D) moyamoya (n=29) patients. Data were quantified in different regions based on anatomical atlases: GM=total gray matter; WM=total white matter; CAU=caudate; CER=cerebellum; FRN=frontal gray matter; INS=insula; OCC=occipital gray matter; PAR=parietal gray matter; PUT=putamen; TMP=temporal gray matter; THL=thalamus. *P<0.05; **P<0.0045 (Bonferroni-corrected P-value; comparisons=11).

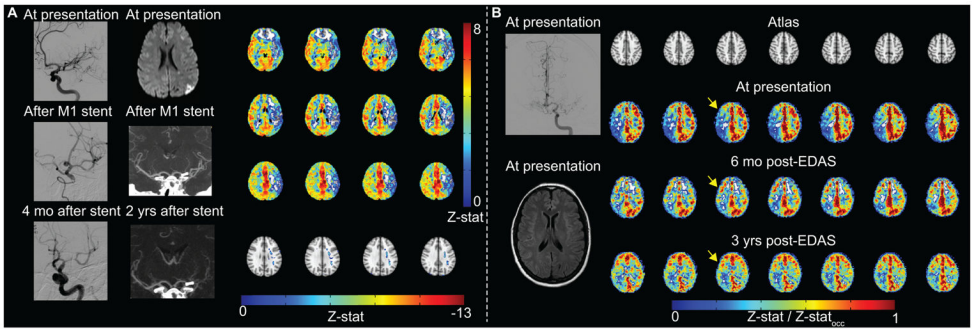

Figure 4. Example patient images

(A) Atherosclerotic patient example. Digital subtraction angiography (DSA) demonstrates severe left M1 stenosis, which is successfully treated with stent placement. Four months after stent placement, in-stent restenosis is significant. Diffusion weighted imaging (DWI) demonstrates watershed infarcts related to severe M1 stenosis. After stent placement, lumenal stenosis is not directly evaluated by computed tomography angiography, but is inferred from decreased opacification of left M2 branches. Blood oxygenation level-dependent (BOLD) cerebrovascular reactivity (CVR) was performed two years after stent placement, when angioplasty was considered due to patient's increasing dysarthria. CVR is markedly reduced in the left MCA territory with negative z-statistic. (B) Moyamoya patient example. Pre-operatively, although DSA from left internal carotid artery (ICA) injection demonstrates bilateral moyamoya disease (mSS=3 on right; mSS=2 on left), and only prior infarct is in left caudate head on FLAIR, BOLD CVR is markedly reduced in the right cerebral hemisphere, thus indirect revascularization with encephaloduroarteriosynangiosis (EDAS) was performed on the right. Revascularization response is demonstrated on CVR images over a three-year duration. Responses have been normalized by occipital Z-statistics ($Z\text{-stat}_{occ}$) to allow for comparison between time points.

Table 1

Volunteer demographics.

	N (Patients)	Age (yrs)	Sex (M/F)	Anti-platelet (Fraction)	Anti-coagulant (Fraction)	Cardiovascular Risk Factors (Fraction)	Diabetes (Fraction)	Smoking (Fraction)	Presence of Infarct (Fraction)
Healthy Control	10	33.1±8.5	5/5	0.00	0.00	0.00	0.10	0.10	0.00
BOLD vs. CBF Reactivity	57	51.2±16.5	22/35	0.88	0.09	0.84	0.35	0.42	0.93
Lateralizing CVR									
Total	60	51.7±15.7	22/38	0.81	0.06	0.79	0.29	0.29	0.79
Atherosclerotic*	31	59.8±13.2	15/16	0.73	0.12	0.91	0.36	0.48	0.85
Moyamoya**	29	41.8±12.7	7/22	0.90	0.00	0.66	0.21	0.21	0.72

Safety	N (Patient Scans)	Age (yrs)	Sex (M/F)	Athero-sclerotic (Fraction)	Moyamoya (Fraction)	Other (Fraction)	Stroke-related symptoms (Fraction)	Other symptoms (Fraction)	Follow-up duration (median;days)
Immediate follow-up	125	50.6±16.0	53/72	0.35	0.52	0.13	0.00	0.02	0.00
Longer-term Follow-up	125	50.6±15.6	53/72	0.35	0.52	0.13	0.05	0.27	372

*For multivariate analysis, asymmetry between affected and contralateral CVR (t-statistic) was used (i.e., n=31 measurements).

**For multivariate analysis, to minimize over-fitting concerns, each hemisphere was considered separately (n=58) and hemisphere modified Suzuki Score added as a predictor. See Supplementary Material for details.

Table 2

Results of multi-variate analysis.

	B±s.e.	T-statistic	P-value
Atherosclerotic (n=31 t-statistics)			
Predictor			
Age(continuous)*	−0.44±0.20	−2.2	0.035
Smoker(dichotomous)	1.2±5.0	0.24	0.813
Diabetes(dichotomous)	4.9±5.1	0.95	0.352
Moyamoya (n=58 hemispheres)			
Predictor			
mSS(categorical)*	−0.90±0.23	−3.9	<0.001
Age(continuous)	−0.037±0.022	−1.7	0.102
Smoker(dichotomous)	0.037±0.69	0.054	0.957
Diabetes(dichotomous)	−0.27±0.79	−0.33	0.739

* Significant predictor at P<0.05.